Methodol Comput Appl Probab (2014) 16:485–506
DOI 10.1007/s11009-013-9363-6

Two Sample Tests for Mean 3D Projective Shapes from Digital Camera Images

Vic Patrangenaru · Mingfei Qiu · Marius Buibas

Received: 14 July 2012 / Revised: 12 June 2013 /
Accepted: 14 July 2013 / Published online: 14 August 2013

Abstract In this article, we extend mean 3D projective shape change in matched pairs to independent samples. We provide a brief introduction of projective shapes of spatial configurations obtained from their digital camera images, building on previous results of Crane and Patrangenaru (J Multivar Anal 102:225–237, 2011). The manifold of projective shapes of k-ads in 3D containing a projective frame at five given landmark indices has a natural Lie group structure, which is inherited from the quaternion multiplication. Here, given the small sample size, one estimates the mean 3D projective shape change in two populations, based on independent random samples of possibly different sizes using Efron's nonparametric bootstrap. This methodology is applied in three relevant applications of analysis of 3D scenes from digital images: visual quality control, face recognition, and scene recognition.

Keywords 3D scene reconstruction from a pair of uncalibrated camera views · 3D projective shape · Quaternions · Fréchet means · Extrinsic mean change on a Lie group · Asymptotic statistics on manifolds · Nonparametric bootstrap on manifolds · Computational statistics · Visual quality control · Face recognition

AMS 2000 Subject Classifications Primary 62H11; Secondary 62H10 · 62H35

Vic Patrangenaru's research supported by National Science Foundation Grants DMS-0805977 and DMS-1106935. Mingfei Qiu's research supported by National Science Foundation Grant DMS-1106935.

V. Patrangenaru (✉) · M. Qiu
Department of Statistics, Florida State University, Tallahassee, FL, USA
e-mail: vic@stat.fsu.edu

M. Qiu
e-mail: mingfeiqiu@stat.fsu.edu

M. Buibas
Brain Corporation, San Diego, CA, USA
e-mail: buibas@braincorporation.com

1 Introduction

Without exception, seers including insects, cephalopods, and vertebrates have bilateral vision. Light from the surrounding environment is gathered and projected onto a pair retinas, where it is translated into electrical impulses and sent to brain regions for further processing. The mechanism of 3D vision within the bounded domain of a brain or of a machine is very complex and, until recently, was poorly understood. On the Geometry and Optics level, progress was made due to key results in Computer Vision by Longuet-Higgins (1981), Faugeras (1992), Hartley et al. (1992) and others. These results, and human visual perception led (Patrangenaru et al. 2012) to conclude that *all we see are 3D projective shapes*.

On the heels of these results, the main objective of this paper is to develop two sample tests statistics for extrinsic 3D mean projective shapes, based on data extracted from pairs of digital camera images. Our methodology is nonparametric bootstrap. Combining bilateral images into a 3D object is a crucial step. Therefore in Section 2 we recall the result on the 3D projective scene reconstruction of a finite spatial configuration from pairs of its *uncalibrated* digital camera images. Here we also introduce $P\Sigma_m^k, k > m + 1$, the projective shape space of k-ads including a projective frame at fixed given indices, and using projective coordinates, we identify this space with a direct product of real projective spaces in dimension m. Analysis of projective shapes regarded as objects, is given as an example of the general Fréchet principle of studying nonlinear data on metric spaces. The distance used between projective shapes is the chord distance via the Veronese–Whitney (VW) embedding of $(\mathbb{R}P^m)^{k-m-2}$ in a product of spaces of symmetric matrices. The VW *mean of a random projective shape* is its *Fréchet mean* relative to this extrinsic distance. Asymptotic test statistics for the equality of the extrinsic means of independent random objects (r. o.'s) on a manifold embedded in the Euclidean space on manifolds were first considered in Hendriks and Landsman (1998) and more recently in Bhattacharya (2008) and Bhattacharya and Bhattacharya (2012). In an attempt of addressing the case of matched pairs, Bhattacharya (2008) also derived a large sample test statistic under the more general assumption of correlated pairs of r. o.'s when the sample sizes are equal. In Section 3, we derive an asymptotic test statistics for the average *change* between two r.o.'s on Lie groups, thus extending hypothesis testing problems for the mean difference of two random vectors to the case of extrinsic means of independent r.o.'s on a Lie group. A two sample hypothesis testing problem for extrinsic means on the embedded manifold $\mathcal{M}$ that admits a simply transitive Lie group of isometries $\mathcal{G}$, can be formulated, and in Theorem 3.1 a large sample test statistic is given for this problem. Nonparametric bootstrap confidence regions are also given in this section. In Section 4 we show that the space of 3D projective shapes of configurations that include a projective frame has a Lie group structure (see also Crane and Patrangenaru 2011), thus allowing to define and test for VW-mean projective shape change. Here we combine previous nonparametric inference methodology for projective shapes with those in Section 3. As a result, nonparametric bootstrap confidence regions for the change in VW 3D means are derived in Corollary 4.1 and Remark 4.2. Section 5 is dedicated to three applications of the nonparametric bootstrap methodology for two samples tests for mean VW 3D projective shapes developed in the previous section. Here we give one example of two sample tests for 3D mean projective shape of polyhedral scenes extracted from digital images, where the null hypothesis is rejected. The 3D projective shape data is extracted from pairs of digital images by combining algorithms described in Ma et al. (2006) and Mardia and Patrangenaru (2005). The first application can be used in visual quality control (see Bhattacharya et al. 2012), the second one in landmark based face recognition, and the third one in scene recognition (a bust of Epicurus). The bust data, which is new, is given for convenience in the Appendix.

2 3D Projective Shapes from Uncalibrated Camera Images and Projective Shape Manifolds

In this section we recall basic facts about the geometry of 3D vision from bilateral views. For more details, see Hartley and Zisserman (2004), Patrangenaru et al. (2010) and the references therein. A point in the outer space and its central projection via the camera pinhole, determine a unique line in space, leading to the definition of the real projective plane $\mathbb{R}P^2$ as space of all straight lines going through the origin of $\mathbb{R}^3$. Consider a real vector space V, and let 0_V be the zero of this vector space. Two vectors $x, y \in V\backslash\{0_V\}$ are equivalent if they differ by a scalar multiple. The equivalence class of $x \in V\backslash\{0_V\}$ is labeled $[x]$, and the set of all such equivalence classes is the *projective space* $P(V)$ associated with V, $P(V) = \{[x], x \in V\backslash\{0_V\}\}$. The real projective space in m dimensions, $\mathbb{R}P^m$ is the projective space $P(\mathbb{R}^{m+1})$. Another notation for a *projective point* $p = [x] \in \mathbb{R}P^m$, equivalence class of $x = (x^1, \ldots, x^{m+1}) \in \mathbb{R}^{m+1}$, is $p = [x^1 : x^2 : \cdots : x^{m+1}]$ featuring the *homogeneous coordinates* of p. The *affine coordinates relative to the last homogeneous coordinate* of the projective point $p = [x^1 : x^2 : \cdots : x^{m+1}]$ are

$$\varphi_{m+1}(p) = (a^1, a^2, \ldots, a^m), a^j = \frac{x^j}{x^{m+1}}, \forall j = 1, \ldots, m. \tag{2.1}$$

The *spherical representation* of a point $[x] \in \mathbb{R}P^m$, is $z = \frac{x}{\|x\|}$, and is uniquely determined up to its sign. A *projective transformation* is a map $\pi : P(V) \to P(V)$, given by $\pi([x]) = [Ax]$, $A \in GL(V)$.

The problem of the reconstruction of a configuration of points in 3D from two ideal uncalibrated camera images with unknown camera parameters, is equivalent to the following: given two camera images $\mathbb{R}P^2_1, \mathbb{R}P^2_2$ of unknown relative position and internal camera parameters and two matching sets of labeled points $\{p_{a,1}, \ldots, p_{a,k}\} \subset \mathbb{R}P^2_a$, $a = 1, 2$, find all the sets of points in space $p_1, \ldots, p_k$ in such that there exist two positions of the planes $\mathbb{R}P^2_1, \mathbb{R}P^2_2$ and internal parameters of the two cameras c_a, $a = 1, 2$ with the property that the c_a-image of p_j is $p_{a,j}$, $\forall a = 1, 2$, $j = 1, \ldots, k$.

In absence of registration errors, in the uncalibrated case, the solution to the reconstruction problem is unique up to a projective transformation (see Faugeras 1992 and Hartley et al. 1992).

Definition 2.1 Two sets of labeled points $\{p_{a,1}, \ldots, p_{a,k}\} \subset \mathbb{R}P^m_a$, $a = 1, 2$, have the same projective shape if there is a projective transformation $\beta : \mathbb{R}P^m \to \mathbb{R}P^m$, such that $\beta(p_{1,j}) = p_{2,j}, \forall j = 1, \ldots k$.

The reconstruction algorithm was therefore reformulated as follows by Sughatadasa (2006) and by Patrangenaru et al. (2010):

Theorem 2.1 *In absence of occlusions, any two 3D reconstructed configurations $\mathcal{R}, \mathcal{R}'$ obtained from a pair of 2D matched configurations in uncalibrated cameras images of a 3D configuration $\mathcal{C}$, have the same projective shape.*

Note that the solution of the reconstruction problem, from a pair of $2D$ images depends on a landmark correspondence.

2.1 Projective Frames and Projective Shapes

A projective frame in $\mathbb{R}P^m$ is an ordered $m+2$ tuple of points $\pi = (p_1, \ldots, p_{m+2})$, any $m+1$ of which are in general position. The *standard* projective frame π_0 is the projective frame associated with the standard vector basis $e = (e_1, \ldots, e_{m+1})$, of $\mathbb{R}^{m+1}$, in this case $\pi_0 = (p_{0,1}, \ldots, p_{0,m+2})$, where $p_{0,j} = [e_j], \forall j = 1, \ldots, m+1$, and $p_{0,m+2} = [e_1 + \cdots + e_{m+1}]$. Note that since the action of a projective transformation is uniquely determined by its action on a projective frame (see Mardia and Patrangenaru 2005), given a point $p \in \mathbb{R}P^m$, its *projective coordinates* p^π *w.r.t. a projective frame* $\pi = (p_1, \ldots, p_{m+2})$ are defined as the image of p under the projective transformation that takes π to π_0 (for an example of projective shape data registration in 2D given in Buibas et al. (2012) see Fig. 1). The projective coordinates of a point on the projective space w.r.t. a projective frame, as well as their equations, in terms of the coordinates of the projective frame are given in Patrangenaru (2001), Mardia and Patrangenaru (2005), Munk et al. (2008), or Patrangenaru et al. (2010).

2.2 Manifolds of Projective Shapes in General Position and their Veronese–Whitney Embeddings

Two ordered sets of points in $\mathbb{R}P^m$ (k-ads) $(p_1, \ldots p_k), (p'_1, \ldots p'_k)$ have the same **projective shape** if there is a projective transformation π of $\mathbb{R}P^m$, with $\pi(p_i) = p'_i, \forall i = 1, \ldots, k$. Having the same projective shape is an equivalence relationship on the set of k-ads, and the equivalence class $p\sigma(p) = p\sigma((p_1, \ldots p_k))$ of a k-ad

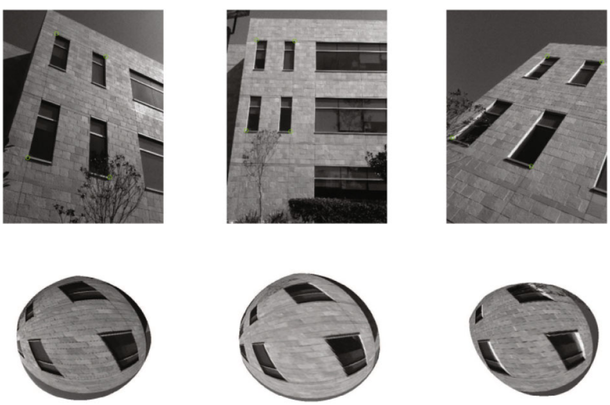

Fig. 1 Original 2D scene and its registered projective coordinates in their spherical representation

$(p_1, \ldots p_k)$ is called *projective shape*. Early statistical studies of projective shape including Mardia et al. (1996), Goodall and Mardia (1999), based on parametric models for projective invariants, were soon replaced by nonparametric data analysis on manifolds using a general method of projective frames by Patrangenaru (1999). There is a particular interest in projective shapes of k-ads *in general position* in $\mathbb{R}P^m$. These are projective shapes of k-ads that contain a projective frame, and in particular for such k-ads $k \geq m+2$. In general, if a configuration of (possibly infinitely many) points contains a projective frame, then the projective shape of that configuration, is determined by the projective coordinates of the other points of this configuration w.r.t. that projective frame. Let $P\Sigma_m^k$ be the set of projective shapes of generic k-ads in $\mathbb{R}P^m$, such that the first $m+2$ points in the k-tuple form a projective frame. $P\Sigma_m^k$ is a manifold diffeomorphic with $(\mathbb{R}P^m)^{k-m-2}$, leading to a *multivariate axial data analysis* (Mardia and Patrangenaru 2005). Assume $q = k - m - 2$. Patrangenaru (2001), Mardia et al. (2003), Mardia and Patrangenaru (2005) and others considered the diagonal equivariant *Veronese–Whitney (VW) embedding* of $P\Sigma_m^k$ given by

$$j_k : P\Sigma_m^k = (\mathbb{R}P^m)^q \to (Sym(m+1))^q \tag{2.2}$$

defined by

$$j_k([x_1], ..., [x_q]) = (j([x_1]), ..., j([x_q])), \tag{2.3}$$

where $x_s \in \mathbb{R}^{m+1}, x_s^T x_s = 1, \forall s = 1, ..., q$ and j is the Veronese–Whitney embedding

$$j([x]) = xx^T, x^T x = 1. \tag{2.4}$$

2.3 Fréchet's Program for a Statistical Analysis of Random Objects

In general, the question of studying random elements (often called *random objects* (r.o.'s)) other than random vectors was first raised by Fréchet (1948). As examples, Fréchet suggested to analyze the shape of a random contour, or the shape of an egg selected at random from an wire egg basket. Fréchet's approach to *Analysis of Object Data* (AoOD) consists in identifying an object with a point in a metric space (M, d). Next, given a r.o. X on M, he defined what we call today the *Fréchet function* on M, given by $F_d(p) = E(d^2(X, p))$. A minimizer of F_d above is a *Fréchet mean*, and the minimum value of F_d is the *Fréchet total variance*. In this paper we follow Fréchet's approach for inference on the projective shape manifold $M = P\Sigma_m^k$ with the distance $d(p\sigma(p), p\sigma(p')) = \| j_k(p\sigma(p)) - j_k(p\sigma(p'))\|$, where $P\Sigma_m^k$ is identified with $(\mathbb{R}P^m)^q$ and j_k is the VW embedding in Eq. 2.4. In this case the Fréchet mean of a random projective shape will be simply called *mean projective shape.* An early study of the asymptotic distribution of the total sample Fréchet variance associated with this distance d is due to Patrangenaru (1999, 2001).

3 Two-Sample Tests for Extrinsic Means on a Lie Group

Recall that a group $(\mathcal{G}, \odot)$ that has in addition an m dimensional manifold structure, such that the group multiplication $\odot : \mathcal{G} \times \mathcal{G} \to \mathcal{G}$, and the inversion $I : \mathcal{G} \to \mathcal{G}$, $I(g) = g^{-1}$ are differentiable maps between manifolds, is called a *Lie group*. For a comprehensive introduction to manifolds and Lie groups, including *tangent spaces and tangent maps associated to differentiable maps between manifolds, embedding,* *the tangent and normal component of a vector, relative to the tangent space at the point of a manifold, vector field on a manifold, Lie algebra of a Lie group, exponential map in a Lie group, etc* see Spivak (1979). Recall that a *local frame field on an m dimensional manifold* $\mathcal{G}$, is an ordered set of local vector fields $(e_1, \ldots, e_m)$ on an open subset $U, e_i : U \to TU$, such that for any point $u \in U$, $(e_1(u), \ldots, e_m(u))$ is a basis of $T_uU = T_u\mathcal{G}$.

3.1 Test for Mean Change in Matched Pairs on a Lie Group

For a large sample of observations from a matched pair (X, Y) of random vectors in $\mathbb{R}^m$, one may estimate the difference vector $D = Y - X$ to eliminate much of the influence of extraneous unit to unit variation (Johnson and Wichern 2007, p. 274), without increasing the dimensionality. Crane and Patrangenaru (2011) extended this technique to paired r.o.'s on an embedded Lie group that is not necessarily commutative. Assuming X and Y are paired r.o.'s on a Lie group $(\mathcal{G}, \odot)$. The *change from X to Y* was defined to be r. o. $C =: X^{-1} \odot Y$. A test for no mean change from X to Y is one for the null hypothesis

$$H_0 : \mu_J = 1_{\mathcal{G}}, \tag{3.1}$$

where $1_{\mathcal{G}}$ is the identity of $\mathcal{G}$ and μ_J is the *extrinsic mean* of C with respect to an embedding $J : \mathcal{G} \to \mathbb{R}^N$, which is given by

$$\mu_J = J^{-1}(P(\mu)). \tag{3.2}$$

Here μ is the mean of $J(C)$ and $P(\mu)$ is its projection on $J(\mathcal{G})$, the point on $J(\mathcal{G})$ that is closest to μ, which is assumed to be unique (C is J-nonfocal). We assume $J(C)$ has finite moments of sufficiently high order. If $C_1, \ldots, C_n$ are i.i.d.r.o. s on $\mathcal{G}$, their extrinsic sample mean is the extrinsic mean of their empirical distribution.

Assume $(e_1, \ldots, e_m)$ is a local orthonormal frame field defined on an open neighborhood $J(U)$ of $P(\mu)$ in $J(\mathcal{G})$ T.he coordinates of the tangential component $tan(v)$ of $v \in \mathbb{R}^N$ w.r.t. the basis $e_a(P(\mu)) \in T_{P(\mu)}J(\mathcal{G}), a = 1, \ldots, m$ are given by

$$tan(v) = (e_1(P(\mu))^T v \ \ldots \ e_m(P(\mu))^T v)^T. \tag{3.3}$$

We set $f_a(u) = (d_uJ)^{-1}(e_a(J(u))), \forall u \in U$. Then the random vector $(d_{\mu_J})^{-1}(tan(P(\overline{J(X)}) - P_j(\mu)))$ has the following covariance matrix w.r.t. the basis $f_1(\mu_J), \cdots, f_m(\mu_J)$:

$$\begin{aligned}\Sigma_J &= (e_a(P(\mu))^T \Sigma_\mu e_b(P(\mu)))_{1 \le a,b \le m} \\ &= \left[\sum d_\mu P(e_b) \cdot e_a(P(\mu))\right]_{a=1,\ldots,m} \Sigma \left[\sum d_\mu P(e_b) \cdot e_a(P(\mu))\right]^T_{a=1,\ldots,m},\end{aligned} \tag{3.4}$$

where Σ is the covariance of $J(C)$ in $\mathbb{R}^N$.

Definition 3.1 The distribution Q (of X_1) is J-nonfocal, if $P(\mu)$ is well defined. The matrix Σ_J given by Eq. 3.4 is the *extrinsic covariance matrix* of the J-nonfocal distribution Q w.r.t. the basis $f_1(\mu_J), \ldots, f_m(\mu_J)$.

Given the i.i.d.'s matched pairs $(X_i, Y_i) \in \mathcal{G}^2, i = 1, \ldots, n$, and the corresponding changes $C_i = X_i^{-1} Y_i \in \mathcal{G}, i = 1, \ldots, n$, it is known (see Bhattacharya and Patrangenaru 2005) that

$$\sqrt{n} tan(J(\bar{C}) - J(\mu_J)) \xrightarrow{\mathcal{L}} \mathcal{N}_m(0, \Sigma_J), \tag{3.5}$$

where Σ_J is the extrinsic covariance matrix of C, and $tan(v)$ is the tangential component in $T_{\mu_{a,J}} J(\mathcal{G})$ of a vector $v \in \mathbb{R}^N$ with respect to the decomposition $\mathbb{R}^N = T_{\mu_{a,J}} J(\mathcal{G}) \oplus (T_{\mu_{a,J}} J(\mathcal{G}))^{\perp}$.

Let $S_{J,n}$ be the sample extrinsic covariance matrix, obtained from the i.i.d.r.o.'s $\{X_r\}_{r=1,\ldots,n}$ from the unknown distribution Q. At this point we recall from Bhattacharya and Patrangenaru (2005) the steps that one takes to obtain a bootstrapped statistic from a pivotal statistic. If $\{X_r^*\}_{r=1,\ldots,n}$ is a random sample from the empirical $\hat{Q}_n$, conditionally given $\{X_r\}_{r=1,\ldots,n}$, then the studentized vector valued statistic

$$V(X, Q) = n^{\frac{1}{2}} S_{J,n}^{-\frac{1}{2}} tan(P(\overline{J(X)}) - P(\mu)) \tag{3.6}$$

leads to the bootstrapped statistic

$$V^*(X^*, \hat{Q}_n) = n^{\frac{1}{2}} S^*_{J,n}{}^{-\frac{1}{2}} tan_{P(\overline{J(X)}))} (P_J(\overline{J(X^*)}) - P_J(\overline{J(X)})). \tag{3.7}$$

Here $S^*_{J,n}$ is obtained from $S_{J,n}$ substituting $X_1^*, \ldots.., X_n^*$ for $X_1, \ldots., X_n$, and $T(X^*, \hat{Q}_n)$ is obtained from $T(X, Q)$ by substituting $X_1^*, \ldots.., X_n^*$ for $X_1, \ldots., X_n$, $\overline{J(X)}$ for μ and $S^*_{J,n}$ for $S_{J,n}$.

Corollary 3.1 *A* $(1 - \alpha)100$ % *bootstrap confidence region for* μ_J *is* $C^*_{n,\alpha} := J^{-1}(U^*_{n,\alpha})$ *with* $U^*_{n,\alpha}$ *given by*

$$U^*_{n,\alpha} = \{\mu \in J(\mathcal{G}) : n \| S_{J,n}^{-\frac{1}{2}} tan(P(\overline{J(X)}) - P(\mu)) \|^2 \leq c^*_{1-\alpha}\}, \tag{3.8}$$

where $c^*_{1-\alpha}$ *is the upper* $100(1 - \alpha)$ % *point of the values*

$$n \| S^*_{J,n}{}^{-\frac{1}{2}} tan_{P(\overline{J(X)})} (P(\overline{J(X^*)}) - P(\overline{J(X)})) \|^2 \tag{3.9}$$

among the bootstrap resamples.

3.2 Two-Sample Tests for Extrinsic Means on Manifolds and Simply Transitive Lie Group Actions

Recall that given an embedding $J : \mathcal{M} \to \mathbb{R}^N$, we consider the *chord distance* on $\mathcal{M}$, given by $d(x_1, x_2) = d_0(J(x_1), J(x_2))$, where d_0 is the Euclidean distance in $\mathbb{R}^N$. If $X_{aj_a} : j_a = 1, \ldots, n_a, a = 1, 2$ are i.i.d.r.o.'s drawn from distributions $Q_a, a = 1, 2$ on a $\mathcal{M}$, if we denote by μ_a the mean of the induced probability $Q_a \circ J^{-1}$ and by Σ_a its covariance matrix $(a = 1, 2)$, then the extrinsic mean of Q_a is $\mu_{a,J} = J^{-1}(P(\mu_a))$, assuming Q_a is J-nonfocal, and the extrinsic sample mean is $\bar{X}_{a,J} = J^{-1}(P(\bar{Y}_a))$. Here, again, P is the projection from $\mathbb{R}^N$ to $J(\mathcal{M})$, and we write $Y_{aj_a} = J(X_{aj_a}) j_a = 1, \ldots, n_a, a = 1, 2$ then $\bar{Y}_a, a = 1, 2$ is the corresponding sample mean. Assuming finite second moments of $Y_{a1}, a = 1, 2$, which is automatic if $\mathcal{M}$ is compact, from Eq. 3.5 we have

$$\sqrt{n_a} tan(J(\bar{X}_{a,J}) - J(\mu_{a,J})) \xrightarrow{\mathcal{L}} \mathcal{N}_m(0, \Sigma_{a,J}), a = 1, 2, \tag{3.10}$$

where $\Sigma_{a,J}$ is the extrinsic covariance matrix of Q_a, and $tan(v)$ is the tangential component in $T_{\mu_{a,J}} J(\mathcal{M})$ of a vector $v \in \mathbb{R}^N$ with respect to the decomposition $\mathbb{R}^N = T_{\mu_{a,J}} J(\mathcal{M}) \oplus (T_{\mu_{a,J}} J(\mathcal{M}))^{\perp}$.

Definition 3.2 An action of a Lie group $\mathcal{G}$ on a manifold $\mathcal{M}$, is a differentiable function $\alpha : \mathcal{G} \times \mathcal{M} \to \mathcal{M}$, such that

$$\begin{aligned} &\alpha(1_{\mathcal{G}}, x) = x, \forall x \in \mathcal{M}, \\ &\alpha(g, \alpha(h, x)) = \alpha(g \odot h, x), \forall g \in \mathcal{G}, \forall h \in \mathcal{G}, \forall x \in \mathcal{M}. \end{aligned} \tag{3.11}$$

$\mathcal{M}$ has a simply transitive Lie group of isometries $\mathcal{G}$, if there is a Lie group action $\alpha : \mathcal{G} \times \mathcal{M} \to \mathcal{M}$ by isometries with the property that given $x \in \mathcal{M}$, for any object $y \in \mathcal{M}$, there is a unique $g \in \mathcal{G}$ such that $\alpha(g, x) = y$.

A two sample hypothesis testing problem for extrinsic means on the embedded manifold $\mathcal{M}$ that admits a simply transitive Lie group of isometries $\mathcal{G}$, can be formulated as follows:

$$\begin{gathered} H_0 : \mu_{2,J} = \alpha(\delta, \mu_{1,J}) \\ \text{versus} \\ H_1 : \mu_{2,J} \neq \alpha(\delta, \mu_{1,J}). \end{gathered} \tag{3.12}$$

Given a fixed object $x \in \mathcal{M}$, the mapping $\alpha^x : \mathcal{G} \to \mathcal{M}, \alpha^x(g) = \alpha(g, x)$ is bijective, therefore the hypothesis problem (Eq. 3.12) is equivalent to the following hypothesis testing problem for a given element δ on the Lie group $\mathcal{G}$:

$$\begin{gathered} (1)\quad H_0 : (\alpha^{\mu_{1,J}})^{-1}(\mu_{2,J}) = \delta, \\ \text{versus} \\ H_1 : (\alpha^{\mu_{1,J}})^{-1}(\mu_{2,J}) \neq \delta \end{gathered} \tag{3.13}$$

Let $H : \mathcal{M}^2 \to \mathcal{G}$, defined by

$$H(x_1, x_2) = (\alpha^{x_1})^{-1}(x_2). \tag{3.14}$$

Theorem 3.1 *Assume X_{a,j_a}, $j_a = 1, \ldots, n_a$ are identically independent distributed random objects (i.i.d.r.o.'s) from the independent probability measures Q_a, $a = 1, 2$ with finite extrinsic moments of order s, $s \leq 4$ on the m dimensional manifold $\mathcal{M}$ on which the Lie group $\mathcal{G}$ acts simply transitively. Let $n = n_1 + n_2$ and assume $\lim_{n\to\infty} \frac{n_1}{n} \to \pi \in (0, 1)$. Let $\varphi : \mathfrak{g} \to \mathcal{G}$ and L_δ be respectively, a chart with $\varphi(1_{\mathcal{G}}) = 0_{\mathfrak{g}}$, and the left translation by $\delta \in \mathcal{G}$. Then under H_0,*

(i.) *The sequence of random vectors*

$$\sqrt{n}(\varphi \circ L_\delta^{-1}(H(\bar{X}_{n_1,J}, \bar{X}_{n_2,J}))) \tag{3.15}$$

converges weakly to $\mathcal{N}_m(0_m, \Sigma_J)$*, for some covariance matrix* Σ_J *that depends linearly on the extrinsic covariance matrices* $\Sigma_{a,J}$ *of* Q_a, $a = 1, 2$.

(ii.) *If (i.) holds and* Σ_J *is positive definite, then the sequence*

$$n(\varphi \circ L_\delta^{-1}(H(\bar{X}_{n_1,J}, \bar{X}_{n_2,J})))^T \Sigma_J^{-1}(\varphi \circ L_\delta^{-1}(H(\bar{X}_{n_1,J}, \bar{X}_{n_2,J}))) \tag{3.16}$$

converges weakly to χ^2_m *distribution.*

The following result is a direct consequence of Cramer's delta method, applied to functions between embedded manifolds.

Lemma 3.1 *Assume* $F : \mathcal{M}_1 \to \mathcal{M}_2$ *is a differentiable function between manifolds. For* $a = 1, 2$, *assume dim* $\mathcal{M}_a = m_a$, *and* $J_a : \mathcal{M}_a \to \mathbb{R}^{N_a}$ *is an embedding. Let* X_n *be a sequence of r.o.'s on* M_1 *such that*

$$\sqrt{n} tan_{J_1(\nu)}(J_1(X_n) - J_1(\nu)) \xrightarrow{\mathcal{L}} \mathcal{N}_{m_1}(0, \Sigma), \tag{3.17}$$

then

$$\sqrt{n} tan_{J_2(F(\nu))}(J_2(F(X_n)) - J_2(F(\nu))) \xrightarrow{\mathcal{L}} \mathcal{N}_{m_2}(0, d_\nu F \Sigma (d_\nu F)^T), \tag{3.18}$$

where $d_\nu F : T_\nu \mathcal{M}_1 \to T_{F(\nu)}\mathcal{M}_2$ *is the differential of* F *at* μ.

Proof of Theorem 3.1 By the inverse function theorem, the mapping $H : \mathcal{M} \times \mathcal{M} \to \mathcal{G}$ is continuous. Given that, according to Bhattacharya and Patrangenaru (2003), for $a = 1, 2$, the extrinsic sample mean $\bar{X}_{n_a,J}$ is a consistent estimator of $\mu_{a,J}$, for $a = 1, 2$, by the continuity theorem (Billingsley 1995, p. 334) a consistent estimator for $(\alpha^{\mu_{1,J}})^{-1}(\mu_{2,J})$ is $H(\bar{X}_{n_1,J}, \bar{X}_{n_2,J})$. From Bhattacharya and Patrangenaru (2005), for $a = 1, 2$,

$$\sqrt{n_a} tan_{\mu_{a,J}}(J(\bar{X}_{n_a,J}) - J(\mu_{a,J})) \xrightarrow{\mathcal{L}} N_m(0_m, \Sigma_{a,J}), \tag{3.19}$$

and, since $\frac{n_a}{n} \to \pi$, it follows that

$$\sqrt{n} tan_{(\mu_{1,J},\mu_{2,J})}(J^2((\bar{X}_{n_1,J}, \bar{X}_{n_2,J})) - J^2((\mu_{1,J}, \mu_{2,J}))) \xrightarrow{\mathcal{L}} N_{2m}(0_{2m}, \Sigma), \tag{3.20}$$

where

$$\Sigma = \begin{pmatrix} \frac{1}{\pi}\Sigma_{1,J} & 0 \\ 0 & \frac{1}{1-\pi}\Sigma_{2,J} \end{pmatrix}. \tag{3.21}$$

We apply Lemma 3.1 to the function $F : \mathcal{M}^2 \to \mathcal{G}$, given by $F = L_{\delta^{-1}} \circ H$, and select a convenient chart φ, and obtain Eq. 3.15. Theorem 3.1(ii.) is an immediate consequence of part (i.) plus a weak continuity argument (Billingsley 1995, p. 334) □

Corollary 3.2 *For* $a = 1, 2$, *assume* x_{a,j_a}, $j_a = 1, \ldots, n_a$, *are random samples from a* J*-nonfocal distribution* Q *on the* m *dimensional embedded manifold* $\mathcal{M}$ *on which the Lie group* $\mathcal{G}$ *acts simply transitively.*

Let $n = n_1 + n_2$, and assume $\lim_{n\to\infty} \frac{n_1}{n} \to \pi \in (0, 1)$. Assume Σ_J is positive definite and $\hat{\Sigma}_J$ is a consistent estimator for Σ_J. The asymptotic p-value for the hypothesis testing problem in Eq. 3.12 is given by $p = P(T \geq t_\delta^2)$ where

$$t_\delta^2 = n((\varphi \circ L_\delta^{-1}(H(\bar{x}_{n_1,J}, \bar{x}_{n_2,J})))^T(\hat{\Sigma}_J)^{-1}(\varphi \circ L_\delta^{-1}(H(\bar{x}_{n_1,J}, \bar{x}_{n_2,J}))), \tag{3.22}$$

and T has a χ_m^2 distribution.

If the distributions are unknown and the samples are small, an alternative approach is to use Efron's nonparametric bootstrap (Efron 1982). If $\max(n_1, n_2) \leq \frac{m}{2}$, the sample mean $\hat{\Sigma}_J$ in Corollary 3.2 does not have an inverse, and pivotal nonparametric bootstrap methodology can not be applied. In this case one may use a nonpivotal bootstrap methodology for the two sample problem H_0 (see Bhattacharya and Ghosh 1978, Hall and Hart 1990, Fisher et al. 1996 or Hall 1997).

Theorem 3.2 *Under the hypotheses of Theorem 3.1i., assume in addition, that for $a = 1, 2$ the support of the distribution of $X_{a,1}$ and the extrinsic mean $\mu_{a,J}$ are included in the domain of the chart φ and $\varphi(X_{a,1})$ has an absolutely continuous component and finite moments of sufficiently high order. Then the joint distribution of*

$$V = \sqrt{n}(\varphi \circ L_\delta^{-1}(H(\bar{X}_{n_1,J}, \bar{X}_{n_2,J})))$$

can be approximated by the bootstrap joint distribution of

$$V^* = \sqrt{n}(\varphi \circ L_\delta^{-1}(H(\bar{X}^*_{n_1,J}, \bar{X}^*_{n_2,J})) \tag{3.23}$$

with an error $O_p(n^{-\frac{1}{2}})$, where, for $a = 1, 2$, $\bar{X}^*_{n_a,J}$ are the extrinsic means of the bootstrap resamples X^*_{a,j_a}, $j_a = 1, \ldots, n_a$, given X_{a,j_a}, $j_a = 1, \ldots, n_a$.

Remark 3.1 Beran and Fisher (1998) were the first to use group actions in hypothesis testing problems, a technique later used in Mardia and Patrangenaru (2005). The drawback in Mardia and Patrangenaru (2005) was that their analysis led to an increase in dimensionality, forcing the extrinsic covariance matrices to be degenerated. In this paper we consider in particular the case when $\mathcal{M}$ itself has a Lie group structure $\odot$, and the group action is left translations: $\alpha : \mathcal{M}^2 \to \mathcal{M}, \alpha(g, x) = g \odot x$. Given two objects x, y the *change from x to y* is $c = x^{-1} \odot y$. Given two random objects X, Y, from Theorem 3.1 we may estimate the change from the extrinsic mean of X to the extrinsic mean of Y. Note that this is the mean change defined in Crane and Patrangenaru (2011) only if X, Y are matched pairs and on a commutative group $(\mathcal{G}, \odot)$.

Remark 3.2 The methodology of simply transitive groups on manifolds can be also adapted to hypothesis testing for two intrinsic means on manifolds, as shown in Osborne et al. (2013)

4 Two Sample Test for VW means of 3D Projective Shapes

In this section we apply the results in Section 3 along with previous results in projective shape analysis, to two sample tests on the projective shape space $P\Sigma_3^k$.

4.1 A Lie Group Structure on the Manifold of 3D Projective Shapes of Configurations Containing a Projective Frame

Note that, as shown by Crane and Patrangenaru (2011), unlike in other dimensions, the projective shape manifold $P\Sigma_3^k, k \geq 5,$ has a Lie group structure, derived from the quaternion multiplication. Recall that if a real number x is identified with $(0, 0, 0, x) \in \mathbb{R}^4$, and if we label the quadruples $(1, 0, 0, 0)$, $(0, 1, 0, 0)$, respectively $(0, 0, 1, 0)$ by $\overrightarrow{i}$, $\overrightarrow{j}$, respectively $\overrightarrow{k}$, then the multiplication table given by

$\odot$	$\overrightarrow{i}$	$\overrightarrow{j}$	$\overrightarrow{k}$
$\overrightarrow{i}$	-1	$\overrightarrow{k}$	$-\overrightarrow{j}$
$\overrightarrow{j}$	$-\overrightarrow{k}$	-1	$\overrightarrow{i}$
$\overrightarrow{k}$	$\overrightarrow{j}$	$-\overrightarrow{i}$	-1

where $a \odot b$ product of a on the first column with b on the top row, is listed on the row of a and column of b, extends by linearity to a multiplication $\odot$ of $\mathbb{R}^4$. Note that $(\mathbb{R}^4, +, \odot)$ has a structure of a noncommutative field, the field of *quaternions*, usually labeled by $\mathbb{H}$. Note that if $h, h' \in \mathbb{H}$, then $\|h \odot h'\| = \|h\|\|h'\|$, and the three dimensional sphere inherits a group structure, the *group of quaternions of norm one*.

Moreover, since $\mathbb{R}P^3$ is the quotient $S^3/x \sim -x$

$$[x] \odot [y] =: [x \odot y], \tag{4.1}$$

is a well defined *Lie group* operator on $\mathbb{R}P^3$, called the group of *p-quaternions*. Note that if $h = t + x\overrightarrow{i} + y\overrightarrow{j} + z\overrightarrow{k}$, its *conjugate* is $\bar{h} = t - x\overrightarrow{i} - y\overrightarrow{j} - z\overrightarrow{k}$, and the inverse of h is given by

$$h^{-1} = \|h\|^{-2}\bar{h}, \tag{4.2}$$

As shown in Section 2, as manifold, $P\Sigma_3^k$ is diffeomorphic with $(\mathbb{R}P^3)^q$, where $q = k - 5$. With this identification, $P\Sigma_3^k \sim (\mathbb{R}P^3)^q$ inherits a Lie group structure from the group structure p-quaternions $\mathbb{R}P^3$ with the multiplication given by

$$\begin{aligned}([h_1], \ldots, [h_q]) \odot ([h'_1], \ldots, [h'_q]) &:= ([h_1] \odot [h'_1], \ldots, [h_q] \odot [h'_q]) \\ &= ([h_1 \odot h'_1], \ldots, [h_q \odot h'_q]).\end{aligned} \tag{4.3}$$

The identity element is given by $1_{(\mathbb{R}P^3)^q} = ([0:0:0:1], \ldots, [0:0:0:1])$, and given a point $\mathbf{h} = ([h_1], \ldots, [h_q]) \in (\mathbb{R}P^3)^q$, from Eq. 4.2, its inverse is $\mathbf{h^{-1}} = \bar{\mathbf{h}} = ([\bar{h}_1], \ldots, [\bar{h}_q])$.

4.2 Nonparametric Bootstrap Tests for VW mean 3D Projective Shape Change

A random projective shape Y of a k-ad in general position including a projective frame in $\mathbb{R}P^m$ has a multivariate axial representation

$$(Y^1, \ldots, Y^q),\ Y^s = [X^s],\ (X^s)^T X^s = 1, \forall s = 1, \ldots, q = k - m - 2. \tag{4.4}$$

Y is VW-nonfocal if $\forall s = 1, \ldots, q$, the largest eigenvalue of $E(X^s(X^s)^T)$ is simple, and, in this case the VW (extrinsic) mean projective shape μ_{j_k} of $(Y^1, \ldots, Y^q)$ is given by

$$\mu_{j_k} = ([\gamma_1(m+1)], ..., [\gamma_q(m+1)]), \tag{4.5}$$

where $\lambda_s(a)$ and $\gamma_s(a), a = 1, \ldots, m+1$ are the eigenvalues in increasing order and the corresponding unit eigenvectors of $E(X^s(X^s)^T)$.

If $Y_r, r = 1, \ldots, n$ are i.i.d.'s from a VW-nonfocal probability distribution on $(\mathbb{R}P^m)^q$, given in their multi-axial representation (Eq. 4.4):

$$Y_r = ([X_r^1], \ldots, [X_r^q]), (X_r^s)^T X_r^s = 1; s = 1, \ldots, q, \tag{4.6}$$

their sample VW-mean can be obtained as follows (see Patrangenaru et al. 2010). Let J_s be the r.o. given by

$$J_s = n^{-1} \Sigma_{r=1}^n X_r^s (X_r^s)^T \quad , \quad s = 1, \ldots, q, \tag{4.7}$$

where $d_s(a)$ and $g_s(a)$ are the eigenvalues in increasing order and corresponding unit eigenvectors of $J_s, a = 1, \ldots, m+1$, then the sample mean VW projective shape, in the multi-axial representation (Eq. 4.4), is given by

$$\overline{Y}_{j_k,n} = ([g_1(m+1)], \ldots, [g_q(m+1)]). \tag{4.8}$$

Mardia and Patrangenaru (2005) showed that if $Y_1, \ldots, Y_n$ are i.i.d.r.o.'s from a VW-nonfocal probability measure on $(\mathbb{R}P^m)^q$ and μ_{j_k} in Eq. 4.5 is the extrinsic mean of Y_1, then the entries of the extrinsic sample covariance matrix $G_n = S_{j_k,n}$ defined in Eq. 4.9, with the pairs of indices $(s, a), s = 1, \ldots, q; a = 1, \ldots, m$, in their lexicographic order, with respect to a convenient orthonormal basis, are given by

$$\begin{aligned} G_{n(s,a),(t,b)} &= n^{-1}(d_s(m+1) - d_s(a))^{-1}(d_t(m+1) - d_t(b))^{-1} \cdot \\ &\quad \cdot \sum_{r=1}^{n} (g_s(a)^T X_r^s)(g_t(b)^T X_r^t)(g_s(m+1)^T X_r^s)(g_t(m+1)^T X_r^t). \end{aligned} \tag{4.9}$$

Moreover, the asymptotic distribution of $\overline{Y}_{j_k,n}$ can be obtained as follows. We consider the matrices D_s given by

$$D_s = (g_s(1) \ldots g_s(m)) \in M(m+1, m; \mathbb{R}), s = 1, \ldots, q. \tag{4.10}$$

If $\mu = ([\gamma_1], \ldots, [\gamma_q])$, where $\gamma_s \in \mathbb{R}^{m+1}, \gamma_s^T \gamma_s = 1$, for $s = 1, \ldots, q$, we define the statistic T:

$$T(\overline{Y}_{j_k,n}; \mu) = n(\gamma_1^T D_1, \ldots, \gamma_q^T D_q) G_n^{-1} (\gamma_1^T D_1, \ldots, \gamma_q^T D_q)^T. \tag{4.11}$$

If Y_1 is a j_k-nonfocal population on $(\mathbb{R}P^m)^q$, and has a nonzero absolutely continuous component, and with $\Sigma_{j_k} > 0$, then the bootstrap distribution of the square norm of the vector valued statistic in Eq. 3.7 is given in our case by

$$\begin{aligned} T(\overline{Y}^*_{j_k}; \overline{Y}_{j_k}) &= n(g_1(m+1)^T D_1^*, \ldots, g_q(m+1)^T D_q^*)\ G_n^{*-1} \\ &\quad \times (g_1(m+1)^T D_1^*, \ldots, g_q(m+1)^T D_q^*)^T. \end{aligned} \tag{4.12}$$

and from Section 3, this statistic is useful in estimation and testing for mean VW-projective shapes. For example for the one sample hypothesis testing problem for mean projective shapes:

$$H_0 : \mu_{j_k} = \mu_0 \text{ vs. } H_1 : \mu_{j_k} \neq \mu_0. \tag{4.13}$$

if $\Sigma_{j_k,n}$ is singular and all the marginal axial distributions have positive definite extrinsic covariance matrices, one may use simultaneous confidence ellipsoids to estimate μ_{j_k}. Assume $(Y_r)_{r=1,\dots,n}$ are i.i.d.r.o.'s from a j_k-nonfocal probability distribution on $(\mathbb{R}P^m)^q$. For each $s = 1, \dots, q$ let Σ_s be the extrinsic covariance matrix of Y_1^s, and let $\overline{Y}^s_{j,n}$ and $G_{s,n}$ be the extrinsic sample mean and the extrinsic sample covariance matrix of the s-th marginal axial and the probability measure of Y_1^s has a nonzero absolutely continuous component w.r.t. the volume measure on $\mathbb{R}P^m$. For $s = 1, \dots, q$ and for $[\gamma_s] \in \mathbb{R}P^m$, $\gamma_s^T \gamma_s = 1$, we consider the statistics:

$$T_s = T_s(\overline{Y}^s_{j,n}, [\gamma_s]) = n\gamma_s^T D_s G_{s,n}^{-1} D_s^T \gamma_s \tag{4.14}$$

and the corresponding bootstrap distributions

$$T_s^* = T_s(\overline{Y}^{s*}_j, \overline{Y}^s_{j,n}) = ng_s(m+1)^T D_s^* {G_{s,n}^*}^{-1} D_s^{*T} g_s(m+1). \tag{4.15}$$

Patrangenaru et al. (2010) showed that T_s has asymptotically a χ^2_m distribution, we obtain the following

Corollary 4.1 *For $s = 1, \dots, q$ let $c^*_{s,1-\beta}$ be the upper $100(1-\beta)$ % point of the values of T_s^* given by Eq. 4.15. We set*

$$C^*_{s,n,\beta} := j^{-1}(U^*_{s,n,\beta}) \tag{4.16}$$

where

$$U^*_{s,n,\beta} = \{\mu_s \in \mathbb{R}P^m : T_s(\overline{y}^s_{j,n}; \mu_s) \leq c^*_{s,1-\beta}\}. \tag{4.17}$$

Then

$$R^*_{n,\alpha} = \prod_{s=1}^{q} C^*_{s,n,\frac{\alpha}{q}} \tag{4.18}$$

with $C^*_{s,n,\beta}$, $U^*_{s,n,\beta}$ given by Eqs. 4.20–4.21 is a region of approximately at least $100(1-\alpha)$ % confidence for μ_{j_k}. The coverage error is of order $O_p(n^{-2})$.

Note that the confidence region in Eq. 4.18 is a product of confidence regions for the VW-means of the marginal axial distributions obtained using a Bonferroni inequality (see Patrangenaru et al. 2010). We apply the Corollaries 4.1, 4.13 to the three dimensional case. The element $([0:0:0:1], \dots, [0:0:0:1])$ in $(\mathbb{R}P^3)^q$, is the unit in our group and is labeled $\mathbf{1_q}$. Given two paired r.o.'s, $\mathbf{H_1}, \mathbf{H_2}$ in their spherical representation on $(\mathbb{R}P^3)^q$, we set $\mathbf{Y} = \bar{\mathbf{H}}_\mathbf{1}\mathbf{H_2}$, and let μ_{j_k} be the extrinsic mean of $\mathbf{Y}$. Then testing the existence of mean 3D projective shape change from $\mathbf{H_1}$ to $\mathbf{H_2}$ amounts to the hypothesis testing problem

$$H_0 : \mu_{j_k} = \mathbf{1_q} \text{ vs. } H_1 : \mu_{j_k} \neq \mathbf{1_q}. \tag{4.19}$$

Assume $(\mathbf{H_{1,r}}, \mathbf{H_{2,r}})_{\mathbf{r=1,\dots,n}}$ are i.i.d.r.o.'s from paired distributions on $(\mathbb{R}P^3)^q$, such that $\mathbf{Y_1} = \bar{\mathbf{H}}_{\mathbf{1,1}}\mathbf{H_{2,1}}$ has a j_k-nonfocal probability distribution on $(\mathbb{R}P^3)^q$. Testing the hypothesis (Eq. 4.19) in the case $m = 3$, at level α, amounts to finding a $1 - \alpha$ confidence region for μ_{j_k} given by Corollary 4.1, and, if the sample is small and the extrinsic sample covariance matrix is degenerate, checking if $\mathbf{1_q}$ is in a $1 - \alpha$ confidence region, amounts to finding the upper $\frac{\alpha}{q}$ cutoffs for the bootstrap distributions of the test statistics $T_s^*, s = 1, \dots, k-5$, and checking if the values of T_s, for $\mu_{j_k} = 1_q$ are all in the corresponding confidence intervals. That is

Remark 4.1 For $m = 3, s = 1, \dots, q = k - 5$ let $c^*_{s,1-\beta}$ be the upper $100(1-\beta)$ % point of the values of T_s^* given by Eq. 4.15. We set

$$C^*_{s,n,\beta} := j^{-1}(U^*_{s,n,\beta}) \tag{4.20}$$

where

$$U^*_{s,n,\beta} = \{\mu_s \in \mathbb{R}P^3 : T_s(\overline{Y}^s_{j,n}; \mu_s) \leq c^*_{s,1-\beta}\}. \tag{4.21}$$

Then

$$R^*_{n,\alpha} = \prod_{s=1}^{q} C^*_{s,n,\frac{\alpha}{q}}, \tag{4.22}$$

with $C^*_{s,n,\beta}, U^*_{s,n,\beta}$ given by Eqs. 4.20–4.21, is a region of approximately at least $100(1-\alpha)$ % confidence for μ_{j_k}. Then we fail to reject at level α the hypothesis that there is a nontrivial mean change in the 3D projective shapes $\mathbf{H_1}, \mathbf{H_2}$ if $\mathbf{1_q} \in \mathbf{R}^*_{\mathbf{n},\alpha}$.

4.3 Two Sample Tests for VW Mean 3D Projective Shapes from Stereo Images

We consider now the case of two sample tests for VW mean projective shapes based on independent samples, using the general tests developed in Section 3. Here $\mathcal{M} = \mathcal{G} = (\mathbb{R}P)^q$, $\delta = \mathbf{1}_q$, $q = k - 5$, and

$$\varphi([x_1], \dots, [x_q]) = (\varphi_{m+1}([x_1]), \dots, \varphi_{m+1}([x_q])). \tag{4.23}$$

In our examples we considered the group action $\alpha : (\mathbb{R}P)^q \times (\mathbb{R}P)^q \to (\mathbb{R}P)^q$ given by the multiplication (Eq. 4.3):

$$\alpha(\mathbf{h}, \mathbf{k}) = \mathbf{h} \odot \mathbf{k}. \tag{4.24}$$

Therefore the hypothesis testing $H_0 : \mu_{1,j_k} = \mu_{2,j_k}$ on the Lie group $((\mathbb{R}P)^q, \odot)$ is equivalent to the testing problem

$$H_0 : \mu_{1,j_k}^{-1} \odot \mu_{2,j_k} = 1_q. \tag{4.25}$$

From Theorem 3.2, if the sample sizes n_1, n_2 are small, it suffices to compute the bootstrap distribution of

$$D^* = \varphi(H(\bar{X}^*_{n_1,j_k}, \bar{X}^*_{n_2,j_k})), \tag{4.26}$$

where $H(\mathbf{h}, \mathbf{k}) = \mathbf{h} \odot \mathbf{k}$ and φ is given by Eq. 4.23.

Remark 4.2 Given that $\varphi(1_q) = \mathbf{0} \in (\mathbb{R}^m)^q$, testing the hypothesis (Eq. 4.25) at level α is equivalent to testing if $\mathbf{0}$ is inside a $100(1-\alpha)$ % bootstrap confidence region for $\varphi(\mu)$. Since the group multiplication in $((\mathbb{R}P)^q, \odot)$ is a product of projective quaternion multiplications (Eq. 4.1), one may use simultaneous bootstrap confidence intervals, based on the q affine marginal bootstrap distributions $(D_1^*, \ldots, D_q^*) = D^*$ in Eq. 4.26. From Bonferroni inequalities, for each $j = j = 1, \ldots, q$, we obtain a $100\left(1 - \frac{\alpha}{q}\right)$ % confidence region C_j^*, that can be visualized as a 3D box, product of three $100\left(1 - \frac{\alpha}{3q}\right)$ % simultaneous confidence intervals.

This is the methodology used in our paper for the last application to image analysis.

5 Applications to 3D Scene Data Analysis

5.1 Analysis of Image Data of Two Polyhedra

We first consider an application for matched pairs of 3D projective shapes from digital images. The theory for such a two sample test (test for mean projective shape change) is developed in Crane and Patrangenaru (2011), where it was applied to stereo medical imaging. Here we consider a toy example consisting in two random samples of polyhedral objects. The first sample, was considered in Patrangenaru et al. (2010), and consists in 16 digital images of a polyhedral surface taken by a uncalibrated digital camera (see Fig. 2).

A second data set of 16 digital images of a related polyhedral scene, that was obtained by a slight modification of the first polyhedral object, is displayed in Fig. 3.

Using the Hartley et al. (1992) algorithm, we obtained the 3D reconstructions from the uncalibrated camera images of the polyhedral surface (Fig. 4). There are 19 landmarks (visible corners), carrying labels as in Patrangenaru et al. (2010), 5 of which form a projective frame. Therefore, in this example the projective shape data is on $P\Sigma_3^{19} = (\mathbb{R}P^3)^{14}$. Using Crane and Patrangenaru (2011), from the bootstrap distribution of Veronese–Whitney sample means, we compute the 14 marginal T^* statistics on the Lie group $\mathbb{R}P^3$.

For $s = 1, \ldots, 14$, the values of the statistics T_s under the null hypothesis are all larger than the corresponding T_s^* for the 95 % simultaneous confidence sets (showed in Fig. 5 as cutoffs) are: $T_1 = 1735771.3$, $T_2 = 2234801.4$, $T_3 = 24260037.4$, $T_4 = 949014.2$, $T_5 = 942757.9$, $T_6 = 148967185.2$, $T_7 = 15847127.4$, $T_8 = 3342761.1$, $T_9 =$

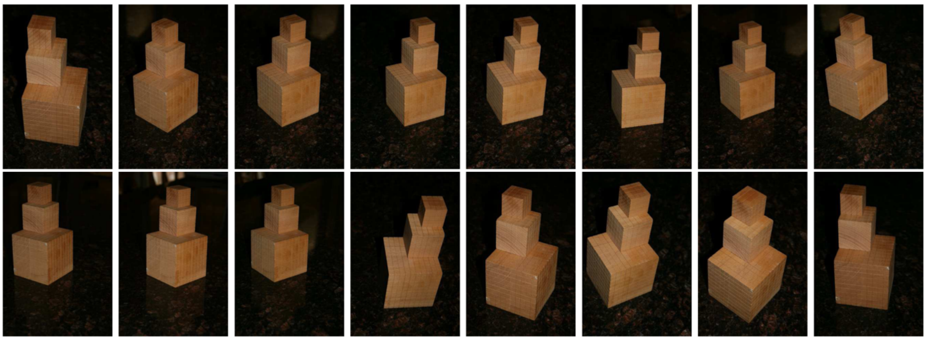

Fig. 2 3D polyhedral surface. Corners are used as landmarks

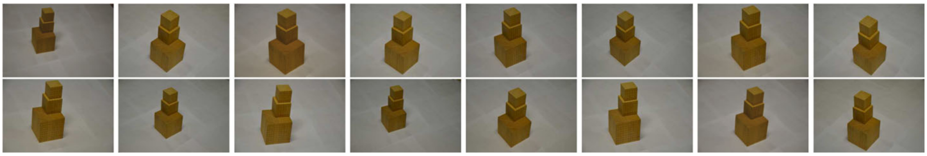

Fig. 3 Top box slightly larger than in Fig. 2

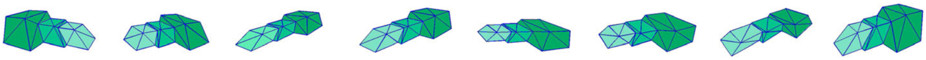

Fig. 4 3D Reconstructions of configurations of corners in Fig. 3

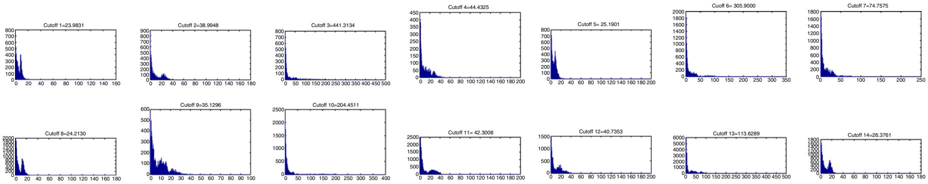

Fig. 5 Cutoffs of the T^* marginal bootstrap statistics

Fig. 6 BBC actor data

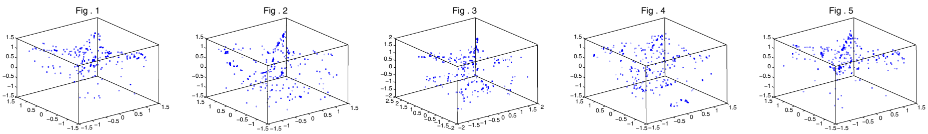

Fig. 7 Simultaneous confidence regions for the mean of the five axial marginals (affine coordinates)

Table 1 Simultaneous confidence affine intervals for mean projective shape change—BBC actor data

Bootstrap simultaneous confidence intervals for facial landmarks 6 to 10					
Coordinate	6	7	8	9	10
x	(−1.26, 1.37)	(−1.28, 1.33)	(−1.56, 1.70)	(−1.29, 1.22)	(−1.43, 1.36)
y	(−1.30, 1.28)	(−1.27, 1.27)	(−1.71, 2.18)	(−1.41, 1.36)	(−1.35, 1.28)
z	(−1.34, 1.18)	(−1.31, 1.20)	(−1.62, 1.86)	(−1.19, 1.27)	(−1.48, 1.23)

Fig. 8 Epicurus bust images

8042772.6, $T_{10} = 15528559.7$, $T_{11} = 3800842.3$, $T_{12} = 35097853.3$, $T_{13} = 24107515.0$, $T_{14} = 7085996.9$.

On the other hand, the corresponding values of the bootstrap cutoffs $T_s^*, s = 1, \ldots, 14$ are: $T_1^* = 23.9831$, $T_2^* = 38.9948$, $T_3^* = 441.3134$, $T_4^* = 44.4325$, $T_5^* = 25.1901$, $T_6^* = 305.9000$, $T_7^* = 74.7575$, $T_8^* = 24.2130$, $T_9^* = 35.1296$, $T_{10}^* = 204.4511$, $T_{11}^* = 42.3008$, $T_{12}^* = 40.7353$, $T_{13}^* = 113.6289$, $T_{14}^* = 26.3761$. The equality of the two population mean projective shapes is rejected at level $\alpha = 0.05$. We infer that the two polyhedral objects are not the same.

5.2 Example 2—Two Sample Test for Means of Independent Pairs

Our data consists in 14 digital camera images of an artist in different disguises (BBC data). The face images data set was used in the context of 2D projective shape in Mardia and Patrangenaru (2005); the need for a 3D projective shape analysis of this data was mentioned in Patrangenaru et al. (2010), where the authors gave a graphic argument for the equality of the mean 3D projective shapes of a group of facial landmarks, from the frontal images, respectively from the one quarter images. We used 8 frontal images, and 6 one quarter images, as shown in Fig. 6. The goal is to test if indeed the projective shape of a 3D configuration of landmarks on the actor's face as extracted from frontal images, is, on average, the same as its projective shape when one quarter views are used in its 3D reconstruction. Figure 10 in the Appendix

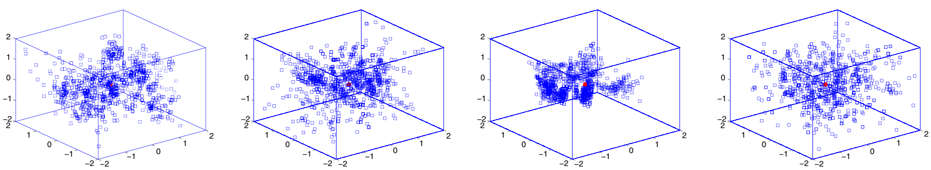

Fig. 9 Simultaneous confidence regions for the statue data

Table 2 Simultaneous confidence affine intervals for mean projective shape change—statue data

Bootstrap simultaneous confidence intervals for statue landmarks 2, 3, 7, 9				
Coordinate	2	3	7	9
x	(−11.52, 11.61)	(−28.65, 30.81)	(−1.96, 1.86)	(−46.36, 42.62)
y	(−11.29, 12.04)	(−32.15, 32.57)	(−1.84, 1.88)	(−47.20, 46.36)
z	(−12.32, 12.49)	(−24.10, 26.31)	(−1.22, 1.41)	(−40.08, 37.08)

displays the actor image with the landmarks used in our analysis, numbered from 1 to 10. The reconstructed 3D configurations are posted at www.stat.fsu.edu/∼vic/MCAP From the 3D configuration of 10 facial landmarks, we selected the landmark 1-5 to construct the projective frame and computed the nonparametric bootstrap distribution of $H(\bar{X}^*_{n_1,j_k}, \bar{X}^*_{n_2,j_k})$ in Eq. 3.23. The affine coordinates of the $10 - 5 = 5$ projective coordinates of the bootstrap VW means for 350 bootstrap resamples are displayed in Fig. 7, and the 95 % confident intervals based on 20,000 bootstrap resamples of each coordinate are displayed in Table 1. Recall from Remark 4.2 that the null hypothesis in this case amounts to all affine coordinates of μ being zero. Since (0, 0, 0) is inside all the 95 % simultaneous marginal confidence affine intervals, listed in Table 4, thus there is insignificant mean projective shape change of the facial landmark configurations between the frontal and one quarter views images. Therefore, we cannot reject the hypothesis that the frontal images and quarter views are from the same person. In order to demonstrate that this allows to identify people, one would need to calculate or simulate the power of the test under the alternative.

5.3 Example 3—Two Sample Test for Means of Half Bust

In this example the data consists in twenty four photos taken of the busts of the Greek philosopher Epicurus. These are displayed in Fig. 8. Sixteen of the images are from a one-head statue, others, in the third row are from a double-head statue, including also one of a disciple of Epicurus. Nine landmarks, displayed in Fig. 10 were selected from the right half of the face of the statues (Fig. 8). The landmark coordinates and the reconstructed 3D configurations obtained from 2D matched configurations in pairs of images are posted at www.stat.fsu.edu/∼vic/MCAP. Landmarks 1, 4, 5, 6, 8 were utilized to construct the projective frame. For the confidence region, we computed 2,000,000 bootstrap VW sample means, based on landmarks 2, 3, 7, 9. For the 4 landmarks, the point (0, 0, 0) is in the 12 simultaneous confidence intervals (see Fig. 9). Therefore based on the given pictures, we fail to reject the null hypothesis that on average the projective shapes of the selected landmark configurations are the same (Table 2).

Acknowledgements The authors are grateful to the anonymous Referees for their excellent constructive comments and suggestions that helped us significantly enhance the quality of the manuscript, that was originally intended only as a computational and applied probability paper.

Appendix

Table 3 displays the registered coordinates of the 19 landmarks in each of sixteen camera images. Camera images paired, each pair was used to reconstruct the 3D polyhedral surface in the Fig. 3.

Table 3 Corner coordinates from paired images in Fig. 3

Landmark no.		1	2	3	4	5	6	7	8	9	10	11	12	13	14	15	16	17	18	19
Image 01	x	2147	1737	1864	2279	1717	1839	2249	1636	1788	2279	1616	1747	2244	1302	1519	2345	1286	1494	2279
	y	162	203	425	380	588	815	765	603	876	810	1023	1302	1241	1074	1580	1454	1697	2218	2092
Image 02	x	2289	1879	2310	2687	1854	2264	2649	1763	2254	2730	1737	2213	2659	1428	2228	2973	1403	2142	2851
	y	253	476	775	512	937	1231	983	1003	1347	1038	1023	1302	1241	1074	1580	1454	1697	2218	2092
Image 03	x	2350	1909	2289	2735	1920	2289	2740	1828	2289	2811	1854	2294	2806	1504	2249	3110	1550	2259	3084
	y	198	395	633	436	912	1140	937	962	1251	998	1535	1839	1560	1712	2259	1778	2598	3160	2659
Image 04	x	2304	1925	2360	2740	1920	2345	2715	1839	2355	2786	1839	2325	2755	1535	2375	3084	1540	2320	3003
	y	304	527	775	527	1013	1241	1003	1059	1362	1064	1600	1889	1580	1808	234	178	2613	3145	2573
Image 05	x	2132	1671	1955	2421	1681	1960	2421	1585	1925	2477	1606	1920	2461	1251	1778	2694	1286	1783	2664
	y	152	294	542	395	770	1028	866	810	1119	927	1337	1651	1459	1464	2041	1687	2279	2867	2487
Image 06	x	1940	1560	1925	2304	1570	1925	2294	1499	1925	2355	1514	1914	2340	1231	1894	2608	1266	1899	2548
	y	309	522	775	557	927	1175	942	988	1292	1008	1418	1732	1443	1616	2198	1646	2244	2781	2304
Image 07	x	2477	1970	2269	2781	1965	2264	2765	1864	2223	2826	1879	2208	2801	1489	2046	3049	1519	2051	3003
	y	56	208	486	324	729	1008	836	760	1109	907	1337	1687	1479	1469	2107	1727	2335	2983	2598
Image 08	x	2396	2021	2467	2846	2051	2487	2836	1965	2497	2917	2011	2502	2902	1732	2568	3241	1793	2563	3176
	y	512	820	1069	760	1241	1489	1180	1307	1621	1236	1752	2061	1687	2006	2598	1904	2634	3191	2517
Image 09	x	2436	1914	2112	2649	1869	2082	2603	1768	2011	2644	1732	1950	2588	1332	1687	2755	1276	1631	2659
	y	46	111	375	304	623	891	826	638	972	886	1226	1570	1474	1292	1899	1722	2198	2836	2639
Image 10	x	2340	1980	2269	2624	1970	2249	2608	1889	2228	2659	1889	2213	2634	1611	2147	2857	1611	2122	2796
	y	360	491	699	562	891	1109	957	932	1195	1003	1373	1636	1449	1504	1996	1646	2168	2659	2299
Image 11	x	2396	1864	2006	2553	1808	1950	2492	1697	1864	2517	1646	1808	2446	1231	1464	2568	1160	1388	2456
	y	248	268	547	517	780	1048	1028	785	1124	1089	1347	1707	1661	1393	2011	1920	2274	2927	2826

Table 3 (continued)

Landmark no.		1	2	3	4	5	6	7	8	9	10	11	12	13	14	15	16	17	18	19
Image 12	x	2153	1773	1965	2350	1757	1940	2330	1676	1904	2370	1676	1879	2340	1383	1722	2492	1383	1712	2446
	y	263	334	562	466	729	937	856	750	1008	896	1170	1433	1327	1241	1727	1519	1894	2391	2158
Image 13	x	2325	1884	2234	2669	1864	2198	2634	1773	2183	2700	1768	2137	2639	1423	2056	2907	1418	2001	2806
	y	370	557	861	663	1003	1297	1109	1043	1423	1175	1524	1894	1636	1687	2365	1899	2391	3059	2578
Image 14	x	2259	1722	1909	2456	1712	1894	2446	1606	1828	2477	1600	1813	2456	1190	1514	2603	1185	1509	2563
	y	122	198	456	370	714	977	896	734	1059	952	1317	1656	1550	1393	1996	1793	2310	2938	2725
Image 15	x	2624	2193	2502	2943	2158	2451	2897	2071	2436	2953	2036	2380	2892	1697	2269	3130	1651	2198	3029
	y	334	456	704	572	927	1170	1038	962	1266	1099	1484	1798	1621	1606	2168	1849	2421	2998	2659
Image 16	x	2122	1788	2228	2558	1803	2249	2548	1737	2254	2629	1752	2259	2618	1499	2360	2958	1524	2345	2907
	y	506	755	942	689	1200	1398	1135	1276	1499	1190	1763	2006	1676	1980	2446	1854	2745	3196	2598

Fig. 10 Landmarks for actor data (*left*) and for Epicurus bust (*right*)

In Fig. 10 the facial landmarks used in our image analysis are marked from 1 to 10. The registered coordinates are displayed in Table 4.

Table 4 Coordinates of facial landmarks for BBC actor data

Landmark →	1	2	3	4	5	6	7	8	9	10
Image↓										
1	265,236	302,232	341,227	377,221	302,179	315,186	328,176	279,149	338,143	303,103
2	299,214	334,210	368,206	400,203	334,161	344,169	358,161	315,134	371,131	338,90
3	266,253	305,251	330,248	365,242	296,209	311,212	321,204	286,185	336,181	308,125
4	201,254	221,250	250,247	228,242	209,203	215,212	233,204	208,179	257,176	234,131
5	264,234	298,234	332,236	361,235	302,194	312,200	321,193	285,165	338,165	302,120
6	367,237	395,227	422,218	449,209	393,182	404,184	412,176	356,167	406,147	365,119
7	327,246	354,244	387,239	416,241	358,206	367,212	377,206	343,176	399,176	365,132
8	273,248	290,248	319,247	353,246	288,211	284,219	305,209	284,179	332,181	304,140
9	269,218	300,219	332,217	365,218	302,170	312,174	328,170	287,150	347,149	314,109
10	197,227	217,232	239,236	275,238	215,188	211,196	231,191	220,159	266,167	244,121
11	304,221	339,216	371,212	401,210	335,169	344,173	359,167	316,149	374,146	338,106
12	247,253	274,252	302,251	335,249	265,211	271,219	284,209	260,182	310,180	281,132
13	282,238	305,236	337,232	367,232	298,191	301,200	316,191	294,161	344,158	314,120
14	346,222	373,218	403,218	435,218	374,172	386,180	398,170	359,146	413,142	378,98

References

Beran R, Fisher NI (1998) Nonparametric comparison of mean axes. Ann Stat 26:472–493

Bhattacharya A (2008) Statistical analysis on manifolds: a nonparametric approach for inference on shape spaces. Sankhya Ser A 70(2):223–266

Bhattacharya RN, Bhattacharya A (2012) Nonparametric statistics on manifolds with applications to shape spaces. In: Institute of mathematical statistics lecture notes–monograph series, vol 3. Cambridge University Press.

Bhattacharya RN, Ellingson L, Liu X, Patrangenaru V, Crane M (2012) Extrinsic analysis on manifolds is computationally faster than intrinsic analysis, with applications to quality control by machine vision. Appl Stoch Model Bus Ind 28:222–235

Bhattacharya RN, Ghosh JK (1978) On the validity of the formal Edgeworth expansion. Ann Stat 6(2):434–451

Bhattacharya RN, Patrangenaru V (2003) Large sample theory of intrinsic and extrinsic sample means on manifolds—part I. Ann Stat 31(1):1–29

Bhattacharya RN, Patrangenaru V (2005) Large sample theory of intrinsic and extrinsic sample means on manifolds—part II. Ann Stat 33(3):1211–1245

Billingsley P (1995) Probability and measure, 3rd edn. Eds Wiley

Buibas M, Crane M, Ellingson L, Patrangenaru V (2012) A projective frame based shape analysis of a rigid scene from noncalibrated digital camera imaging outputs. In: JSM proceedings, 2011, institute of mathematical statistics. Miami, FL, pp 4730–4744

Crane M, Patrangenaru V (2011) Random change on a Lie group and mean glaucomatous projective shape change detection from stereo pair image. J Multivar Anal 102:225–237
Efron B (1982) The Jackknife, the Bootstrap and other resampling plans. In: CBMS-NSF regional conference series in applied mathematics, vol 38. SIAM
Faugeras OD (1992) What can be seen in three dimensions with an uncalibrated stereo rig? In: Proc. European conference on computer vision, LNCS, vol 588, pp 563–578
Fisher NI, Hall P, Jing B-Y, Wood ATA (1996) Improved pivotal methods for constructing confidence regions with directional data. J Am Stat Assoc 91:1062–1070
Fréchet M (1948) Les élements aléatoires de nature quelconque dans un espace distancié. Ann Inst H Poincaré 10:215–310
Ma Y, Soatto S, Kosecka J, Sastry SS (2006) An invitation to 3-D vision. Springer, New York
Goodall C, Mardia KV (1999) Projective shape analysis. J Graph Comput Stat 8:143–168
Hall P (1997) The bootstrap and Edgeworth expansion. Springer Series in Statistics, New York
Hall P, Hart JD (1990) Bootstrap test for difference between means in nonparametric regression. J Am Stat Assoc 85:1039–104
Hartley RI, Gupta R, Chang T (1992) Stereo from uncalibrated cameras. In: Proc. IEEE conference on computer vision and pattern recognition, pp 761–764
Hartley RI, Zisserman A (2004) Multiple view geometry in computer vision, 2nd edn. Cambridge University Press
Hendriks H, Landsman Z (1998) Mean location and sample mean location on manifolds: asymptotics, tests, confidence regions. J Multivar Anal 67(2):227–243
Johnson RA, Wichern DW (2007) Applied multivariate statistical analysis, 6th edn. Prentice Hall
Longuet-Higgins C (1981) A computer algorithm for reconstructing a scene from two projections. Nature 293:133–135
Mardia KV, Goodall C, Walder A (1996) Distributions of projective invariants and model-based machine vision. Adv Appl Probab 28:641–661
Mardia KV, Patrangenaru V (2005) Directions and projective shapes. Ann Stat 33:1666–1699
Mardia KV, Patrangenaru V, Derado G, Patrangenaru VP (2003) Reconstruction of planar scenes from multiple views using affine and projective shape. In: Proceedings of the 2003 workshop on statistical signal processing, pp 285–288
Munk A, Paige R, Pang J, Patrangenaru V, Ruymgaart FH (2008) The one and multisample problem for functional data with applications to projective shape analysis. J Multiv Anal 99:815–833
Osborne D, Patrangenaru V, Ellingson L, Groisser D, Schwartzman A (2013) Nonparametric two-sample tests on homogeneous Riemannian manifolds, Cholesky decompositions and diffusion tensor image analysis. J Multivar Anal 103:163–175
Patrangenaru V (1999) Moving projective frames and spatial scene identification. In: Mardia KV, Aykroyd RG, Dryden IL (eds) Proceedings in spatial-temporal modeling and applications. Leeds University Press, pp 53–57
Patrangenaru V (2001) New large sample and bootstrap methods on shape spaces in high level analysis of natural images. Commun Stat Theory Methods 30:1675–1695
Patrangenaru V, Crane MA, Liu X, Descombes X, Derado G, Liu W, Balan V, Patrangenaru VP, Thompson HW (2012) Methodology for 3D scene reconstruction from digital camera images. In: Proceedings of the international conference of Differential Geometry and Dynamical Systems (DGDS-2011), vol 19, BSG Proceedings, 6–9 October 2011. Bucharest, Romania, pp 110–124
Patrangenaru V, Liu X, Sugathadasa S (2010) Nonparametric 3D projective shape estimation from pairs of 2D images—I, in memory of Dayawansa WP. J Multivar Anal 101:11–31
Spivak M (1979) A comprehensive introduction to differential geometry, vols I–II, 2nd edn. Publish or Perish, Inc., Wilmington, Del
Sughatadasa SM (2006) Affine and projective shape analysis with applications. Ph.D. Dissertation, Texas Tech Univesity